Morphology, structural and optical study of ZnS thin films prepared by Successive Ionic Layer Adsorption and Reaction (SILAR) Method

A. DJELLOUL*, M. ADNANE, Y. LARBAH, S. HAMZAOUI

[a]*Laboratory of Electron Microscopy and Materials Sciences, University of Science and Technology of Oran, BP 1505, El-Mnaouer Oran, 31000, Algeria*

Zinc Sulphide (ZnS) thin films are deposited on glass substrate by relatively simple, quick and cost effective successive ionic layer adsorption and reaction (SILAR) method at room temperature (27°C). For ZnS thin film growth the parameters including concentrations of cationic and ionic precursors, number of immersion cycle, immersion time and pH of the solution are optimized. A further study has been made for structural, surface morphological and optical properties of the film using X-ray diffraction (XRD), EDAX, scanning electron microscopy (SEM), and optical absorption method (UV). The as deposited ZnS thin film exhibited hexagonal phase with optical band gap (Eg) of 3.93 eV. SEM image confirmed that film of smooth surface morphology.

(Received March 04, 2015; accepted February 10, 2016)

Keywords: ZnS, SILAR, XRD, EDAX, SEM, UV.

1. Introduction

Zinc sulphide (ZnS) is an important semiconducting material with a wide direct band gap and n-type conductivity is promising for optoelectronic device applications, such as electroluminescent devices and photovoltaic cells [1-4]. It is of interest for replacement of CdS as buffer layer of thin film based solar cells due to higher energy gap, good transparency, and general good film properties.

Several techniques on growing ZnS thin films have been reported, which include Successive Ionic Layer Adsorption and Reaction (SILAR) [5-8], Sputtering [9], Spray Pyrolysis (SP) [10,11], Chemical Bath Deposition (CBD) [12-18], Molecular Beam Epitaxy (MBE) [19], Dip Technique (DT), Pulsed-Laser Deposition (PLD)[20], Chemical Vapour Deposition (CVD) [21], Metalorganic Chemical Vapour Deposition (MOCVD) [22], Metalorganic Vapour-Phase Epitaxy (MOVPE) [23] and Atomic Layer Epitaxy (ALE) [24].

In this work, we used the SILAR method to produce ZnS thin films.

The SILAR technique, introduced by Nicolau [25], is a unique method in which thin films of compound semiconductors can be deposited by alternate dipping of a substrate into the aqueous solutions containing ions of each component. The SILAR method resembles CBD but deposition control of the growth is easier since the precursors for the cation and anion constituents of the thin film are in different vessels. The growth of thin films in the SILAR method occurs only heterogeneously on the solid–solution interface due to the intermediate rinsing step between the cation and anion immersions. Therefore, the thickness of the film can be controlled simply by the number of growth cycles. The equipment for the SILAR technique can be very simple and inexpensive due to the ambient growth conditions used [25,26]. The deposition conditions were optimized for good quality and well adherent ZnS thin films. These films were characterized for their structural, morphological and optical properties by using X-ray diffraction, Scanning electron microscopy and optical absorption studies.

2. Experimental details

2.1 Preparation of thin film

The deposition was carried out by using Corning glass slides (25mm X 75mm X 1mm) as substrates. The substrates were ultrasonically cleaned with 15% hydrochloric acid, ethanol, acetone and purified deionized water for 30 min, respectively. Zinc acetate zinc dihydrate ($Zn(CH_3COO)_2{\cdot}2H_2O$), thiourea $CS(NH_2)_2$ and liquor ammonia were used for deposition of ZnS thin films were of analytical reagent grade. In the synthesis of ZnS thin film the cationic precursor was 0.1M Zinc acetate solution complexed with ammonia solution at pH=10 for Zinc ion and anionic precursor was 0.1M thiourea solution for sulphide ion. Direct exchange of cationic and anionic ions was modified by means of rinsing in double distilled water. Each SILAR cycle consist of i) adsorption of Zn^{2+} ions from

Zinc acetate solution for 40s, ii) rinsing with double distilled water for 60s, iii) reaction with sulphide precursor solution from thiourea solution for 40s and finally iv) rinsing with double distilled water for 10s. This process was repeated for 50 times to get desired film thickness.

2.2 Characterization of thin film

The structural characterization of the films was carried out using Philips (PW-3710) X-ray diffractometer with CuK_α radiation (α= 1.5404 Å) in 2ϴ range from 20^0-80^0.The surface morphological study of ZnS films was carried out by scanning electron microscopy (SEM) using a model VEGA3 operating at a voltage of 20KV uses the BSE detector and Energy dispersive X-ray analysis (E-DAX) were recorded on Energy dispersive X-ray spectrometer attached to the SEM model.

3. Results and discussion

3.1 The film formation mechanism

The film formation of ZnS thin films by SILAR method are shown in Fig. 1 and Fig. 2.

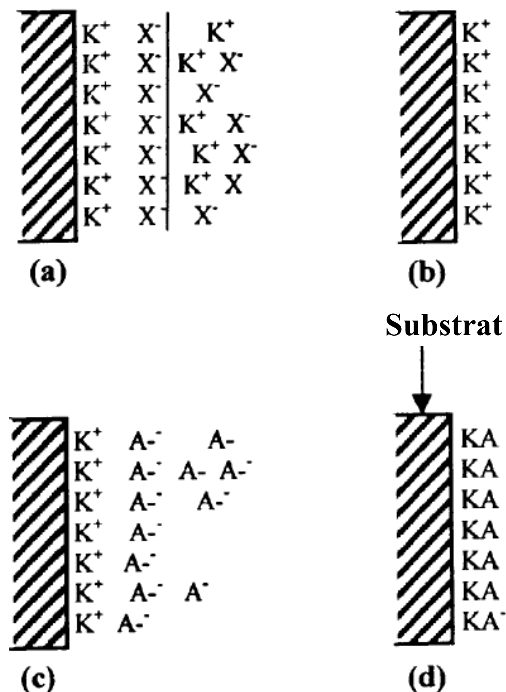

Fig. 1.Diagram SILAR process: (a) adsorption of K^+ X^- and the formation of the double electric layer, (b) rinsing (I)removes the excess of K^+ and X^- unabsorbed, (c) reaction of A^- with the caution K^+ KA reabsorbed to form and (d) rinsing (II)remove excess unreacted species and form the solid to the KA surface of the substrate.

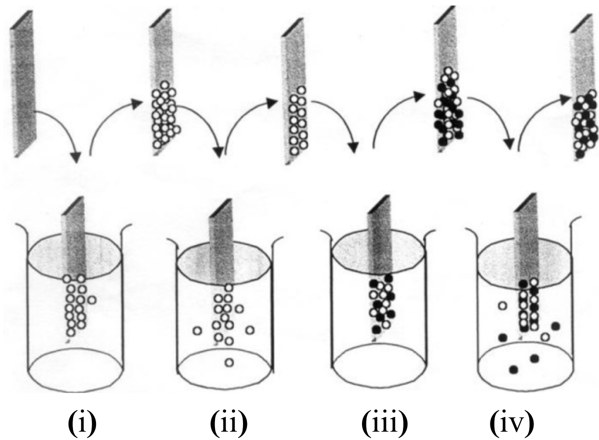

Fig. 2.The scheme of SILAR trend for the deposition of ZnS thin films (O, Zn^{2+};□, S^{2-}) [27].

To deposit ZnS thin film one SILAR cycle involves the following four steps:

i. Adsorption of Zn^{2+}, a well cleaned glass substrate is immersed in the 0.1M Zinc acetate solution having Zn^{2+} zinc ions are adsorbed on glass substrate. ii. Rinsing the unabsorbed Zn^{2+} ions are separated out by dipping the substrate in double distilled water.iii. Reaction with S^{2-}, sulphide ions were adsorbed from an aqueous solution of 0.1 M thiourea. iv. Rinsing finally the substrate was washed with distilled water, thus one SILAR cycle is completed. After few number of such SILAR cycles, ZnS thin film is formed onto glass substrate.

Repeating number of SILAR cycle for different concentrations, immersion cycle and immersion times, preparative parameters for best quality ZnS thin films were optimized as illustrated in Table 1.

Table 1. Optimized preparative parameters for ZnS thin films.

Parameters	Precursors solutions	
	Zinc acetate	Thiourea
Concentration (M)	0.1	0.1
PH	~ 10	~ 10
Immersion time (S)	40	40
Rinsing time (S)	60	60
Number of SILAR cycle	50	50
Temperature (K)	300	300

The variation of ZnS film thickness as a function of number of deposition cycles at constant concentration of Zinc acetate and thiourea is as shown in Fig. 3.

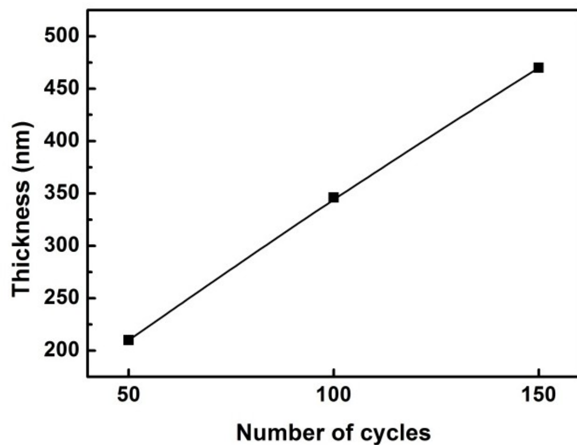

Fig. 3.Variation of ZnS film thickness as a function of number of deposition cycles at constant concentration of Zinc acetate (0.1M) and concentration of thiourea (0.1M).

Initially film thickness increases with deposition time. This ZnS film had maximum terminal thickness of 470 nm for 150 immersion cycle, after this film thickness starts to decrease due to peeling of the material from the substrate.

3.2 Structural studies

In order to study crystal structure of ZnS film deposited by SILAR method, X-ray diffractogram of the film onto glass substrate was examined. Zinc sulphide can be grown with either hexagonal, wurtzite type structure or the cubic zincblende-type structure. Previous reports on chemically deposited ZnS films showed that films were amorphous before annealing while films annealed from 200°C to 400°C were polycrystalline [28]. Fig. 4a shows the XRD pattern of as-deposited film with poor crystallinity, since no well-resolved peaks were observed except a small intensity peaks at 2θ = 30.897° (1 0 1) and 2θ = 59.726° (0 0 4) over a wide base that corresponds to hexagonal phase of ZnS. The low intensity and broad diffraction peak shows that the as-deposited ZnS thin film is nanocrystalline and/or amorphous phase. The low temperature (300 K) at which the ZnS film deposited is responsible for a poor crystallinity, as is often the case. The broad hump (2θ = 15–40°) is due to glass substrate and also possibly due to some amorphous phase of ZnS film. The XRD pattern (Fig. 4b) of film annealed at 400°C for 2 h in air shows the well resolved peaks at 2θ = 27.242° (1 0 0); 2θ = 28.833° (0 0 2) ; 2θ = 30.897° (1 0 1) ; 2θ = 40.083° (1 0 2) ; 2θ = 48.145° (1 1 0) ; 2θ = 58.309° (2 0 1) ; 2θ = 59.726° (0 0 4) and 2θ = 73.894° (2 0 3) , comparison of observed '2θ' with standard '2θ' values confirms that the formed compound is ZnS with hexagonal structure (JCPDS card, no. 80-0007) [29]. The significant improvement in crystallinity is due to sintering of nanocrystals into effectively larger crystals after air annealing. By annealing at higher temperature, further crystallization takes place and crystalline phase prevails over the mixture of amorphous and nanocrystalline one. Average crystallite size of ZnS film was calculated by using the Debye–Scherer formula [30]:

$$D = K.\lambda / \beta.\cos\theta \quad (1)$$

Where:

D: is the mean particle size.

β: is the full width at half maximum (FWHM in radians) of the peak corrected for instrumental broadening, and θ is the diffraction/Bragg's angle.

λ: is the wavelength of the X-ray radiation (0.15406 nm). K: is the Scherer constant, it is value is taken as 0.9 for the calculations [31-33].

The crystallite size of as-deposited film was found to be 8 nm that increases to 15 nm after annealing ZnS thin film at 400°C for 2 h in air that indicates significant improvement in individual crystallite sizes after air annealing.

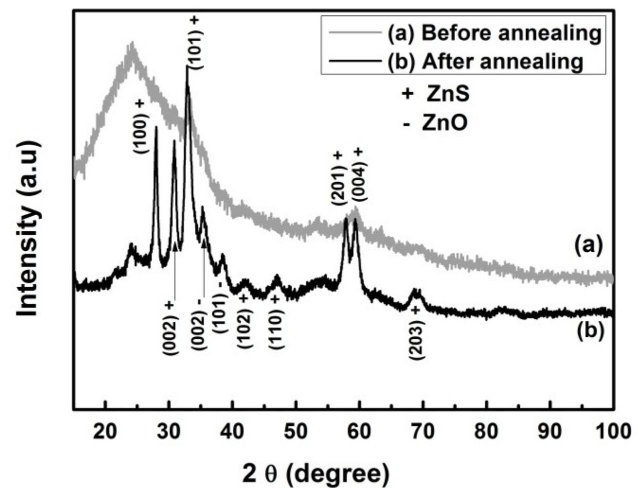

Fig. 4.XRD pattern of ZnS thin film deposited by SILAR method onto glass substrate,a) before annealing and b) after annealing at 400°C in air (2h).

3.3 Surface morphological studies

The scanning electron microscopy technique is familiar for the study of surface morphology of metal chalcogenides in the thin film form.The ZnS film prepared with optimized parameters is used for SEM observation.

Fig. 5 shows the SEM micrograph of ZnS thin film. The film is homogeneous, well adherent and covers glass substrate without cracks and pin hole. The film compactness is high, the grain size is generally small and they are agglomerated in some places.

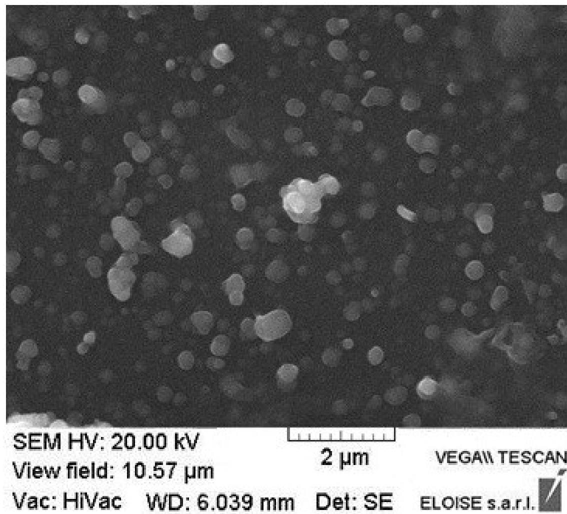

Fig.5.SEM image of as-deposited ZnS film on glass substrate at room temperature.

The E-DAX technique is used to determine quantitative composition of ZnS films deposited on glass substrate. The presence of EDAX peaks for Zn and S are conformed from analysis (figure 6).

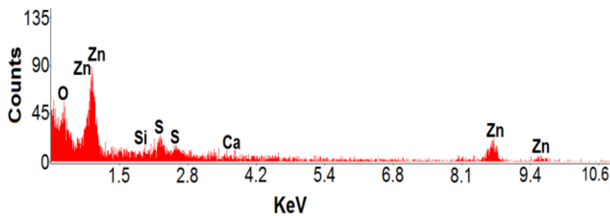

Fig. 6.The EDAX analysis of as- deposited ZnS on glass substrate at room temperature.

The composition ratio was 1.06 of atomic mass percent for Zn and S respectively as shown in Table 2. EDAX spectrum also shows that prepared films are free from impurities. The presences of (O, Si and Ca) are due to glass substrates [35].

Table 2. Elemental analysis of as-deposited ZnS thin film.

Element	**Zn**	**S**	**S/Zn ratio**
Weight %	65.61	34.39	0.52
Atomic %	48. 34	51.66	1.06

3.4 Optical properties

Optical transmission for the as-deposited ZnS thin films on glass substrates were measured in the range (300-800 nm) using a spectrophotometer. The spectral transmittance curves of these films are shown in Fig. 7.

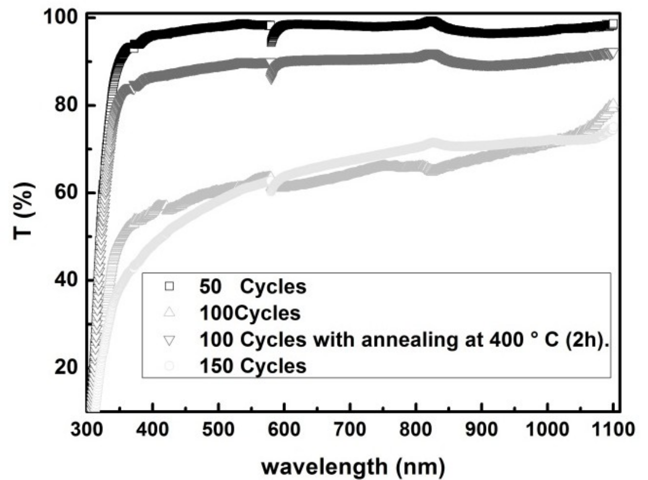

Fig. 7.Absorbance spectra of as-deposited ZnS thin films for different thicknesses on glass substrate at room temperature.

The films present a good transmission. The as-deposited films for 100 cycles present a maximum of transmission (94%). The films for 100 cycles with annealing at 400°C for 2 hours presented increased transmission in the visible range above 85-90%.It can be seen that the ZnS films show high optical transmittance and can be used as buffer layer of CIS solar cells [36-44].This result can be attributed to decreases in thickness; the films were annealed as to change the morphology surface and the stoichiometry of these films.

The absorption coefficient of ZnS thin films was calculated using the transmittance (T) value and thickness d using the relation:

$$\alpha = (\ln (1/T)/d) \tag{2}$$

The absorption coefficient α can be expressed by Urbach relation [45, 46]:

$$\alpha = A\,(h\upsilon - Eg)^{n} / (h\upsilon) \tag{3}$$

Where A is a constant, Eg is the energy gap, υ is the frequency of the incident radiation and h is Planck's constant. The exponent n is 0.5 for direct allowed transitions. ZnS is a direct band gap material; several workers reported this type of transition [47, 48]. The energy gaps of the films of various temperatures have been determined by extrapolating the linear portion of the plots of $(\alpha h\nu)^2$ against hυ (eV) to the energy axis.

The band gap value was determined from the intercept of the straight-line portion of the $(\alpha h\nu)^2$ against the graph on the (hν) axis (see Fig. 8).

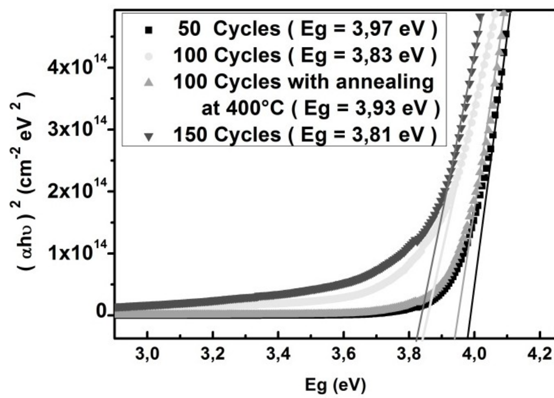

Fig. 8. Plot of $(\alpha h\nu)^2$ versus (hν) of as-deposited ZnS thin films thicknesses on glass substrate at room temperature.

Fig. 8 shows the plot of $(\alpha h\nu)^2$ versus the incident radiation energy (hν) (eV). The band gap value (Eg) calculated from the linear fit of this plot is about 3.93 eV, which is consistent with the literature [4, 11]. It can be seen there is a decrease (from ~3.97 eV to ~3.81 eV) of the band gap for all number of cycles. The estimated band gap values are listed in the table 3.

Table 3. Estimated band gap values.

Number of cycles	Thickness (nm)	Band gap (eV)
50	210	3.97
100	346	3.83
150	470	3.81

It could be observed that for each number of cycles, the optical band gap was decreasing with increasing thickness as shown in Fig. 8 and table 3, because the crystalline quality decreased with increasing thickness of the layer.

The band gap of the as-deposited ZnS thin film was 3.83 eV, which is lower than the band gap of 3.93 eV for ZnS thin film annealed at 400 °C. The band gap of the ZnS thin films changed with annealing temperature, as shown in Fig. 8,this in agreement with the XRD analysis. This tendency is caused by the changes in the crystallite size and the inter-planar distance of the annealed ZnS thin films with increasing annealing temperature. The variation in the band gap as a function of the annealing temperature is coincident with the changes in the crystallite size and the inter-planar distance with annealing temperature. The band gap changes with increasing annealing temperature are thought to be caused by changes in the defects, the composition, the internal strain and the crystalline properties of the ZnS thin film.

Due to the high optical band gap of the ZnS film, it could be useful as buffer layers in CIS thin film solar cells.

4. Conclusions

In this study ZnS thin films were grown on glass substrates by SILAR method with varied number of deposition cycles. The film was characterized for morphological, structural and optical characteristics. The film thickness is dependent on the deposition cycles.

Structural analysis reveals that the deposited films were polycrystalline nature showed hexagonal structure of ZnS thin films and a preferred orientation in the (101) plane after annealing at 400°C in air (2h).The SEM micrograph reveals that substrate is homogeneous, well adherent and covers glass substrate without cracks and pin hole. The grain size is generally small and they are agglomerated in some places. The atomic percentage values of Zn and S derived from the EDAX data confirms the transformation from the disordered state to a relatively ordered state in the film. The optical band gap of ZnS thin film was found to be 3.93 eV. These films can be used as buffer layers in the fabrication of heterojunction thin film solar cells.in this template useful in the preparation of your submission.

Acknowledgements

The authors would like to thank Algerian Ministry of Higher Education and Scientific Research and Directorate General for Scientific Research and Technological Development.

References

[1] S. Yamaga, A. Yoshokawa and H. Kasain, J. Cryst. Growth **86**, 252 (1998).
[2] I.C. Ndukwe, Sol. Energy Mater. Sol. Cells **40**, 123 (1996).
[3] T. E. Varitimos, R. W. Tustison, Thin Solid Films **151**, 27 (1987).
[4] J. Vidal, O. de Melo, O. Vigil, N. Lopez, G. Contreras-Puente, O. Zelaya-Angel, Thin Solid Films **419**, 118 (2002).
[5] M. P. Valkonen, S. Lindroos, T. Kanniainen, M. Leskela, U. Tapper, E. Kauppinen, Appl Surf Sci **120**, 58–64 (1997).
[6] Y. F. Nicolau, J. C. Menard, J Crystal Growth **92**, 128 (1988).
[7] G. Xu, S. Ji, C. Miao, G. Liu, and C. Ye, Journal of Materials Chemistry **22**, 4890 (2012).
[8] H. M. Pathan and C. D. Lokhande, Bull. Mater. Sci **27**, 85 (2004).
[9] H. Murray, A. Tosser. Thin Solid Films **24**, 165 (1974).
[10] H. L. Kwok. J Phys D: Appl Phys **16**, 2367 (1983).
[11] O. M. Hussain, P. S. Reddy, B. S. Naidu, U. Uthanna, P. J. Reddy, Semicond Sci Technol **16**, 690 (1991).
[12] H. Lekiket, M. S. Aida, Mater.Sci.Semicond.Process **16**, 1753 (2013)
[13] P. Roy, J. R. Ota, S. K. Srivastava, Thin Solid Films **515**, 1912 (2006).
[14] T. BenNasr, N. Kamoun, M. Kanzari, R. Bennaceur, Thin Solid Films **500**, 4 (2006).

[15] F. Gōde, C. Gümüs, M. Zor, J.Cryst.Growth **299**, 136 (2007).
[16] G. L. Agawane, S. W. Shin, A. V. Moholkar, K. V. Gurav, J. H. Yun, J. Y. Lee, J. H. Kim, J. Alloys Compd **535**, 53 (2012).
[17] T. Lwushita, S.Z. Shi, Thin Solid Films **520**, 7076 (2012).
[18] Z.Q. Li, J.H. Shi, Q.Q. Liu, Z.A. Wang, Z. Sun, S.M. Huang, Applied Surface Science **257**, 676 (2010).
[19] K. Ichino, T. Onishi, Y. Kawakami, S. Fujita. J Crystal Growth **138**, 28 (1994).
[20] Z.J. Xin, R.J. Peaty, H.N. Rutt, R.W. Eason, Semicond Sci Technol **14**, 695 (1999).
[21] T.L. Chu, S.S. Chu, J. Britt, C. Feredikes, C.Q. Wu, J Appl Phys **70**(5), 2688 (1991).
[22] A. Abounadi, M. D. Blasio, D. Bouchara, J. Calas, M. Averous, O. Briot, N. Briot, T. Cloitre, R. L. Aulombard, B. Gil, Phys. Rev.B **50**, 11677 (1994).
[23] X. M. Fernandez, P. Prete, N. Lovergine, A. M. Mancini, R. Cingolani, L. Vasanelli, M. R. Perrine, Phys.Rev.B **55**, 7660 (1997).
[24] J. Ihanus, M. Ritala, M. Leskelaand, T. Prohaska, R. Resch, G. Friedbacher, et al, Appl Surf Sci **120**, 43 (1997).
[25] Y. F. Nicolaue, Appl. Surf. Sci **1061**, 22 (1985).
[26] S. Lindroos, T. Kanniainen, M. Leskela, Appl Surf Sci **75**, 70 (1994).
[27] H. M. pathan, C. D. Lokhande, Bull. Mater.Sci **27**, 89 (2004).
[28] M. A. Yildirim, A. Ates, A. Astam, Physica E. **41**, 1365 (2009).
[29] C. Yeh, Z.W. Lu, S. Froyen, A. Zunger, Phys. Rev. B: Condens.Matter **46** 10086 (1992).
[30] E. Lifshin, X-ray Charachterization of Materials. (Wiley-VCH, New York, 1999).
[31] S. S. Nath, D. Chakdar, and G. Gope, Nanotrends- A journal of nanotechnology and its application **02**, 03 (2007).
[32] S.S. Nath, D. Chakdar, G. Gope, and D.K. Avasthi, Journal of Nanoelectronics and Optoelectronics **3**, 1 (2008).
[33] B.D. Hall, D. Zanchet and D. Ugarte, Journal of Applied Crystallography **33**, 06 (2000).
[34] R.S. Araoz, Helmholtz-Zentrum Berlin für Materialien und Energie, (Juni 2009).
[35] R. Sahraei, G.M. Aval, A. Goudarzi, Journal of Alloys and Compounds **466**, 488 (2008).
[36] Y. Kouhlane, B. Chouial, S. Gagui, B. Hadjoudja, A. Chibani, Indian J. Phys **88**, 471 (2014).
[37] S.D. Sartale, B.R. Sankapal, M. Lux-Steiner, A. Ennaoui, Thin Solid **Films168**, 480 (2005).
[38] A. Ennaoui, W. Eisele, M. Lux-Steiner, T.P. Niesen, F. Karg, Thin Solid Films **335**, 431 (2003).
[39] J.M. Dona and J. Herrero, J. Electrochem. Soc**141**, 205 (1994).
[40] B. Asenjo, A.M. Chaparro, M.T. Gutierrez, J. Herrero, J. Klaer, Sol. Energy Mater. Sol. Cells **92**, 302 (2008).
[41] B. Asenjo, A.M. Chaparro, M.T. Gutiérrez, J. Herrero, J. Klaer, Thin Solid Films **515**, 6036 (2007).
[42] C. Hubert, N. Naghavi, B. Canava, A. Etcheberry, D. Lincot, Thin Solid Films **515**, 6032 (2007).
[43] T. Miyawaki, M. Ichimura, Mater. Lett61, 4683 (2007).
[44] T. Nakada, M. Hongo, E. Hayashi, Thin Solid Films **242**, 431 (2003).
[45] J. Tauc, A. Meneth, Journal of Non-Crystalline Solids **8-10**, 569–85 (1972).
[46] J.N. Pankove, Optical Processes in Semiconductors, Dover, New York (1971).
[47] A. Antony, K.V. Murali, R. Manoj, and M. K. Jayaraj, Materials Chemistry and Physics **90**, 106 (2005).
[48] A. U. Ubale, V.S. Sangawar and D. K .Kulkarni , Bull. Mater.Sci **30**, 147 (2007).

*Corresponding author: abdelkader.djelloul@gmail.com